Journal of Magnetism and Magnetic Materials 432 (2017) 190–197

Contents lists available at ScienceDirect

Journal of Magnetism and Magnetic Materials

journal homepage: www.elsevier.com/locate/jmmm

Growth of magnetite films by a hydrogel method

A.A. Velásquez [a,*], C.C. Marín [a], J.P. Urquijo [b]

[a] Grupo de Electromagnetismo Aplicado, Universidad EAFIT, A.A. 3300, Medellín, Colombia
[b] Grupo de Estado Sólido, Instituto de Física, Universidad de Antioquia, A.A. 1226, Medellín, Colombia

ARTICLE INFO

Article history:
Received 12 October 2016
Received in revised form 30 November 2016
Accepted 23 January 2017
Available online 4 February 2017

Keywords:
Magnetite films
Hydrogel method
MÖSSBAUER spectroscopy
Vibrating sample magnetometry

ABSTRACT

Magnetite (Fe_3O_4) films were grown on glass substrates by formation and condensation of complex of iron oxides in an agarose hydrogel. The obtained films were characterized by Fourier Transform Infrared Spectroscopy (FTIR), Thermogravimetric Analysis (TGA), Scanning Electron Microscopy (SEM), Room Temperature Mössbauer Spectroscopy (TMS), Vibrating Sample Magnetometry (VSM), Atomic Force Microscopy (AFM) and Voltage vs. Current measurements by the four-point method. FTIR and TGA measurements showed that some polymer chains of agarose remain linked to the surface of the magnetic particles of the films after heat treatment. SEM measurements showed that the films are composed by quasi spherical particles with sizes around 55 nm. Mössbauer spectroscopy measurements showed two sextets with broaden lines, which were assigned to magnetite with a distributed particle size, and two doublets, which were assigned to superparamagnetic phases of magnetite. For the specific dimensions of the films prepared, measurements of Voltage vs. Current showed an ohmic behavior for currents between 0 and 200 nA, with a resistance of 355 kΩ.

1. Introduction

Thin films of iron oxides are materials that have attracted increasing attention due to their broad number of technological applications, such as magneto-resistive systems, magneto-optical systems, Hall effect sensors, among others [1]. Many magnetic materials have been investigated for this kind of applications, but magnetite (Fe_3O_4) and maghemite (γ-Fe2O3) are between most studied compounds because their high magnetic response, half-metallic behavior [2] and spin polarized conductivity through the hopping current between Fe^{3+} and Fe^{2+} ions occupying neighboring octahedra. Different methods for synthesizing thin films from iron oxides have been reported in the literature, among them are: sputtering magnetron [3], Pulsed Laser Deposition (PLD) [4], Chemical Vapor Deposition (CVD) [5], sol gel [6,7] and solid reactions [8]. The wet methods have some advantages over plasma-based methods due to their low cost and the simple instrumentation required, which is accessible to most laboratories for research in materials. In this paper, we present the synthesis and characterization of magnetite films by using an agarose gel as template to control the reaction kinetics. No much information on application of agarose in this kind of systems is available, however this method could be a good alternative for obtaining films of magnetic nanoscale particles at low cost and with easy implementation in the laboratory. We studied some structural, magnetic and electrical properties of these films in order to determine their response to physical stimuli, locking for future applications of these materials as sensing devices. Details on the preparation and characterization of the films are presented in the following sections.

2. Materials and methods

For the growth of the thin films, we used the following analytical grade reagents supplied by Merck: $FeCl_2{\cdot}4H_2O$, $FeCl_3{\cdot}6H_2O$ as precursors of Fe^{2+} and Fe^{3+} ions respectively, agarose as the polymer precursor of the hydrogel which controls the reaction kinetics, NH_4OH as reagent to bring the reaction to the proper pH for the hydrolysis of the iron cations and deionized and deaerated water as solvent. In our experiment, 0.2 mol of $FeCl_3{\cdot}6H_2O$ and 0.1 mol of $FeCl_2{\cdot}4H_2O$ were dissolved in 100 ml of aqueous solution of agarose 1% previously heated at 80 °C. Afterward, square glass substrates with 1 cm side and 1 mm thickness, previously washed with isopropyl alcohol, were deposited horizontally inside a Petri dish. We poured 20 ml of the solution of iron salts and agarose into the Petri dish to reach a height of 3.5 mm, covering totally the substrates, afterward we let rest the solution by 48 h until to obtain a hydrogel. Subsequently we added to the hydrogel an alkaline solution of NH_4OH 0.5 M (100 ml) with pH 12 for promoting the condensation of the magnetite crystals. Finally, we let react the

* Corresponding author.
E-mail address: avelas26@eafit.edu.edu.co (A.A. Velásquez).

http://dx.doi.org/10.1016/j.jmmm.2017.01.098
0304-8853/

alkaline solution with the hydrogel by 48 h until the formation of a black gel was observed. The excess of NH_4OH was removed with successive washes with deionized and deaerated water; then the black gel was submitted to a thermal treatment at 120 °C during one hour into a muffle EDG 3000-Vácuo in air presence with a heating rate of 3 °C/min.

The presence of iron oxides as well as the presence of polymeric groups in the films were studied by FTIR using a Spectrum two – Perkin Elmer equipment, the thermal decomposition of organic compounds present in the films were analyzed by Thermogravimetric Analysis with a Q500 – TA Instruments equipment, using a sample mass of 48.03 mg and a rate heating of 5 °C/min in a $N_{2(g)}$ atmosphere. The morphology and particle size were analyzed with a field emission scanning electron microscope JEOL JSM-6701F, with acceleration voltage of 15 kV and magnifications around 85,000. Surface topography micrographs were performed with an atomic force microscope model easyScan 2 from Nanosurf. The magnetic phases and hyperfine interactions in the particles of the films were studied by room temperature transmission Mössbauer spectroscopy by using a Mössbauer spectrometer developed in our laboratory. This spectrometer operates in mode of constant acceleration, with a radioactive source of $^{57}Co(Rh)$, with initial activity of 25 mCi and velocities between −12 mm/s and 12 mm/s. The absorbers were prepared by detaching the films from the substrates in the form of sheets, and placing them in the sample holder of the spectrometer. The films were separated from the substrates in order to prevent the attenuation of the 14.4 keV gamma rays emitted by the radioactive source by the glass substrate. Magnetization measurements were made with a vibrating sample magnetometer developed in our laboratory, which has a resolution of 3×10^{-4} emu in magnetic moment and a range of 10 kOe in magnetic field. The samples for VSM were prepared by detaching the material of the films and building with it cylinders with 3 mm diameter and 4 mm length, which were placed in the sample holder. The electrical properties of the films were studied through Voltage vs. Current measurements by the four-point method [9]. For these measurements we placed thin copper wire points in the corners of the films with silver paint. Afterward we applied current between two terminals and measured the voltage in the other two terminals. To cancel the contribution of the potential of contact and reduce the noise in the measurements, we reversed the current flow in each voltage measurement and then calculated the semi-difference of the voltages measured. We programmed current ramps with steps of 10 nA by using a KEITHLEY 6221 source. The maximum current applied to the films was limited to 200 nA in order to prevent overheating by Joule effect. The voltage measurements were performed with a nanovoltmeter KEITHLEY 2182A. The two devices were interconnected and then connected to a computer through a communication interface IEEE 488-USB from National Instruments. We automated and controlled all measurements from a computer through a user graphical interface developed in LabVIEW software.

Because no significant differences were observed in the measurements obtained with different films, for sake of brevity, only the results obtained with one of the films are presented in the section of results.

3. Theory

Agarose is a polysaccharide extracted from red algae of the class Rhodophyceae. As presented in Fig. 1, this hydrocolloid is a linear polymer consisting of β-D-Galactopyranosyl units and 3–6 alternate Anhydro-α-L-Galactopyranosyl [10].

In aqueous solution at high temperatures, the polymer chains of agarose have a random coil structure, behaving like a semi-flexible polymer. On cooling the solution, agarose chains form helical turn fibers which aggregate in a rolled structure with radius between 20 to 30 nm. As presented in Fig. 2(a), when the agarose gel completely gelled, it acquires a tridimensional network structure with a pore range between 50 and 200 nm. The mechanism proposed by Tako [11] considers the gelation as formation of intramolecular hydrogen bonds between the OH-4 with axial orientation of the unit β-D-galactopyranosyl and oxygen hemiacetal adjacent unit 3,6 anhydro-α-L-galactopyranosyl, besides the formation of intermolecular bonds between two different units 3,6 anhydro-α-L-ga lactopyranosyl by 3,6 of a unit oxygen and OH-2 group with axial configuration of another unit. The pore size in the gel is related to the concentration of agarose, its melting point and gelling. This structure is composed by the highest density regions, where polymer chains aggregate and surround regions with higher concentrations of solvent corresponding to the pores. It has further been reported [12] dependence between the size of the pores in the gel, the ionic strength and the polymer concentration. High ionic strength promotes the formation of pores larger diameter.

The morphological characteristic of agarose gels allows their use as template for controlled formation of oxides. The three-dimensional pores of this gel act as mini-reactors, where the reaction of the formation of the particles take place in controlled manner, because of limitation of available precursors. The polymer chains which make up the walls of the pores act as barriers between the particles, avoiding their aggregation in the early stages of formation and promoting the homogeneous growth of the crystals.

To employ the agarose as template for the formation of magnetite particles, the precursor salts of Fe^{3+} and Fe^{2+} are diluted in the agarose solution after it is carried out to melting point. When the temperature of the mixture decreases, the product becomes gelled, being the hydrated iron ions trapped mainly in the agarose pores, where the solvent concentration is higher. Afterward, the addition of an alkaline solution to a high pH allows the hydrolysis of the cations Fe^{3+} and Fe^{2+} and the subsequent condensation of iron oxide crystals. Under thermal treatment, the polymer chains as well as the residual solution in the mini-reactors decompose,

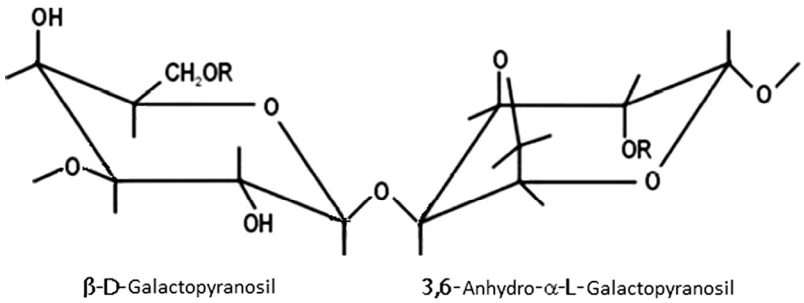

Fig. 1. Chemical structure of agarose.

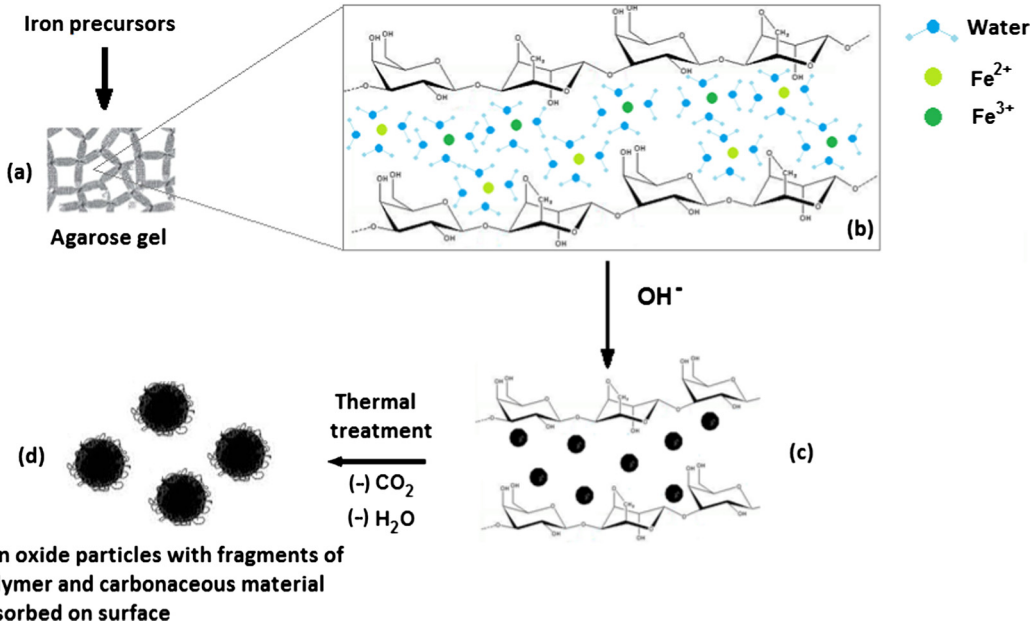

Fig. 2. Mechanism of formation of magnetic iron oxide particles in the agarose structure: a. Agarose template, b. Precursor solution of iron cations in the agarose template, c. Alkaline hydrolysis of the iron cations and formation of the magnetic particles, c. Magnetic particles obtained after thermal treatment.

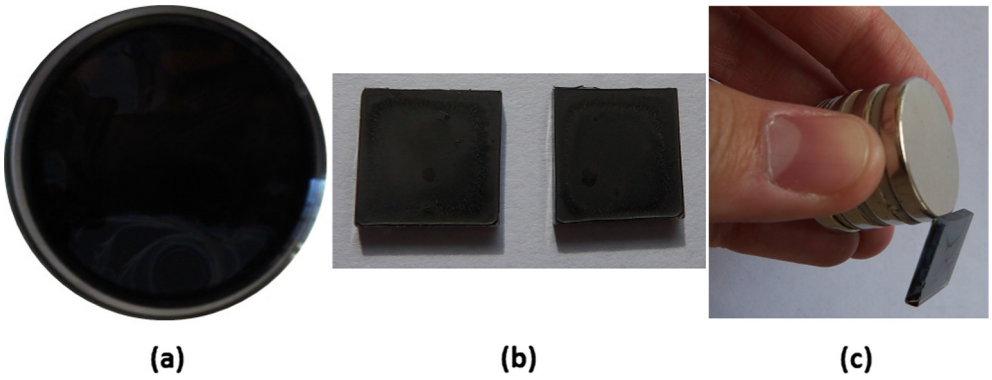

Fig. 3. a. Black gel formed after alkaline hydrolysis of Fe^{2+} and Fe^{3+} in the hydrogel precursor, b. View of the films obtained after thermal treatment, c. Response of the film/substrate to a permanent magnetic field.

being the final product iron oxide particles with polymer and carbonaceous material adsorbed on surface. The Fig. 2 presents the mechanism of formation of the magnetic iron oxide particles in the agarose gel proposed in the present work.

4. Results and discussion

4.1. The films

Fig. 3(a) shows the black gel formed after the reaction of the precursor hydrogel of iron salts with the alkaline solution of NH_3, while Fig. 3(b) shows a view of the films obtained after thermal treatment of the black gel in the muffle. The films were completely adhered to the glass substrates and presented magnetic response to a magnetic field, as evidenced in Fig. 3(c).

4.2. FT-IR measurements

Fig. 4 shows the FTIR spectrum of the aqueous agarose solution, before addition of the iron solutions. The spectrum presents a band around 1070 cm^{-1} characteristic of C–C vibrations in agarose [13]. The band around 1630 cm^{-1} corresponds to molecular vibrations of water, while the broad band around 3300 cm^{-1} corresponds to vibration of O–H groups in water and agarose.

Fig. 5 shows one of the FTIR spectra of the films after thermal treatment. The bands around 407 cm^{-1} and 540 cm^{-1} correspond to the vibrational stretching modes Fe-O in the octahedral and tetrahedral sites of magnetite respectively [14]. The band around 1068 cm^{-1} is attributed to the C–C vibration of residual agarose surrounding the magnetite particles, as a result of the polymer that could not be decomposed during the thermal treatment. The band around 1600 cm^{-1} corresponds to molecular vibrations of water, while the band around 3250 cm^{-1} corresponds to vibration of O–H groups in water and agarose. As we will see later, this result is consistent with the TGA measurements, where is observed that agarose is not totally decomposed during the thermal treatment. The residual polymer present in the films was foreseen by us because polymer chains can bond to the surface of the magnetic nanoparticles by the surface charge present on them, increasing thereby the temperature required for their thermal decomposition. The polymer chains bonded to the surface of the particles do not

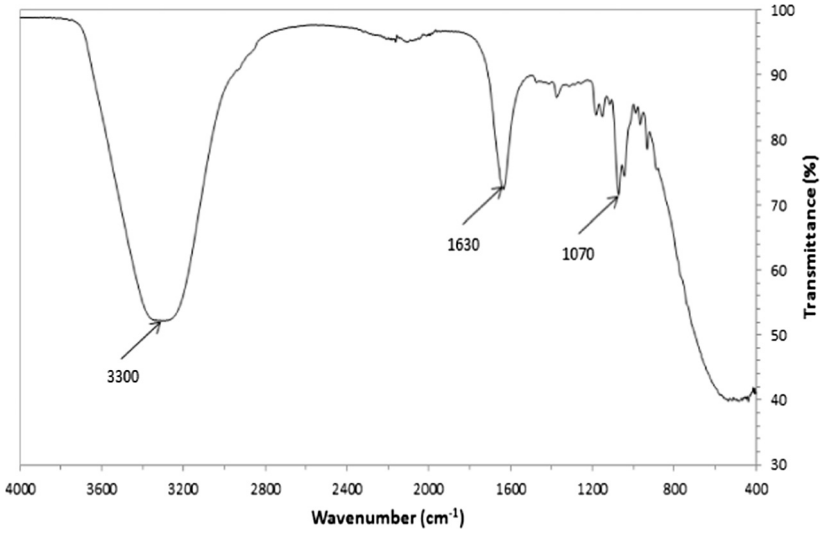

Fig. 4. FTIR of the agarose gel employed in the experiment.

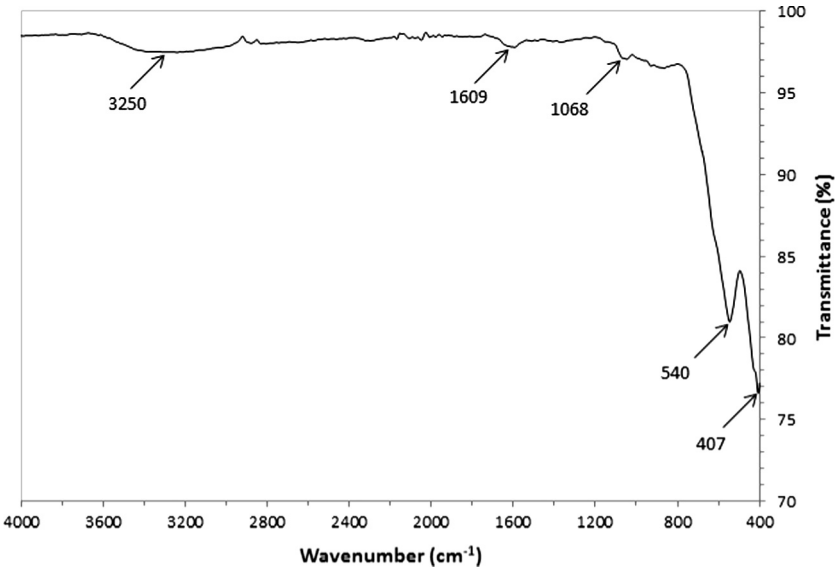

Fig. 5. FTIR spectrum of the film.

represent a problem because they can be used as support media for subsequent functionalization of the films in different applications.

4.3. Thermogravimetric measurements

With the purpose to confirm the decomposition temperature of the agarose, we took first a thermogram of the agarose solution, before addition of the iron solutions, which is presented in Fig. 6. The curve shows one critical weight loss around 96 °C and the derivative of the curve confirms this critical point. This measurement gave us a first criterion to choose the thermal treatment temperature of the films, which was selected at 120 °C. The second criterion to work at 120 °C was to prevent the conversion of magnetite (Fe_3O_4) to maghemite (γ-Fe_2O_3) in the films, looking for preserve their electrical conductivity. According to the literature [15] this conversion can start from 200 °C for synthetic magnetite.

Fig. 7 shows the thermogram of the film, which shows a sharp weight loss around 211 °C, which we attributed to the decomposition of residual agarose aggregated to the magnetic particles. We attribute the second critical weight loss observed around 233 °C to agarose adsorbed on the surface of the magnetite particles. These results confirm that the thermal treatment of the black gel at 120 °C does not allow the total decomposition of the agarose when it is in presence of the magnetic particles, as observed in the FTIR measurements.

4.4. SEM measurements

Fig. 8 shows the micrograph of the film obtained by SEM. From the micrograph it is possible to observe aggregates of particles with quasi spherical shape and with approximate diameter of 55 nm, although smaller particles can also be observed.

4.5. Atomic Force Microscopy measurements

The superficial topography of the film is presented in Fig. 9(a). The image shows a uniform growth of the film, with grains of 4 μm in diameter approximately. These grains are agglomerates

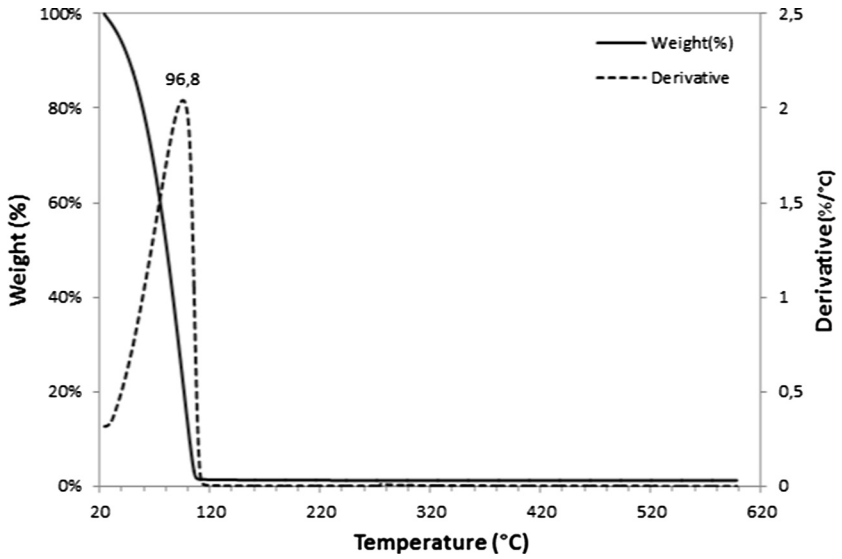

Fig. 6. Thermogram of the agarose solution employed in the preparation of the films.

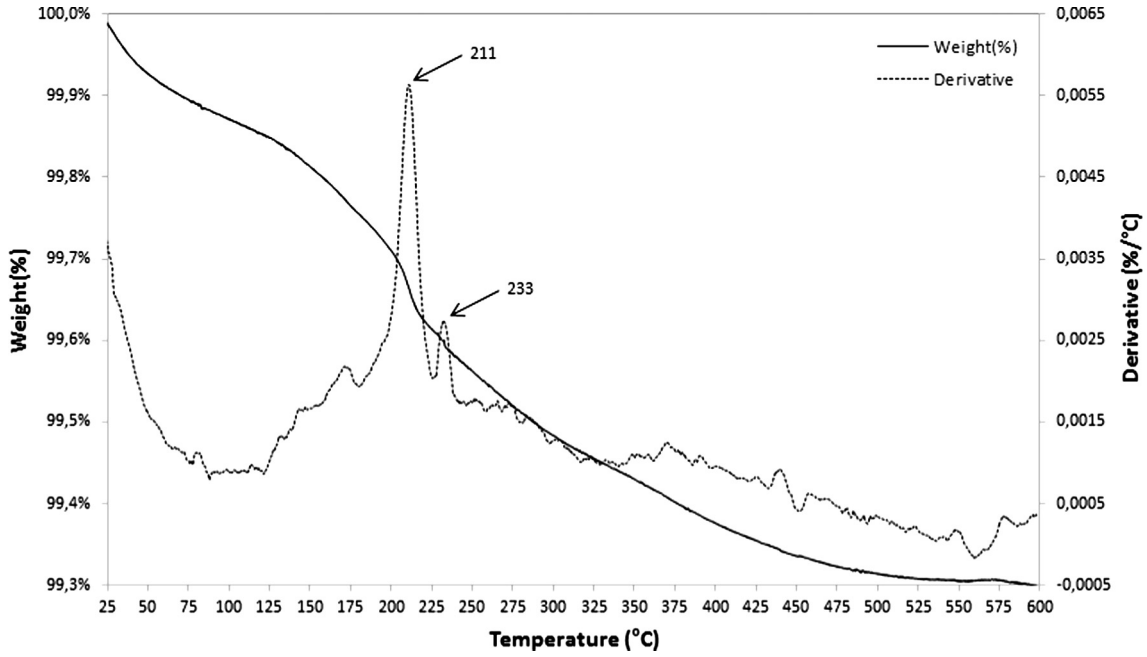

Fig. 7. Thermogram of the film after thermal treatment.

of magnetic particles and the residual polymer linked to them. No cracks are observed in the film, although the dark regions between the grains indicate that the film does not cover totally the surface of the substrate but some aggregates of magnetic particles form during the film growth. The root mean square rugosity of the film was 457 nm. To estimate the thickness of the film, we made a small scratch on its surface with a sharp object until to discover the substrate, subsequently we took the AFM micrograph around this scratch, as presented in Fig. 9(b), which allowed us to estimate an approximate thickness of the film of 3.9 μm.

4.6. Transmission Mössbauer spectroscopy

The room temperature Mössbauer spectrum of the film is presented in Fig. 10 and the Table 1 shows the hyperfine parameters obtained from the fitting of the Mössbauer spectrum with the software by least squares MOSFIT [16]. All spectral parameters remained free during the fitting process. The spectrum was well fitted with two sextets of broaden Lorentzian lines, which have hyperfine parameters of Fe^{3+} and $Fe^{2.5+}$ ions of magnetite, and two doublets with hyperfine parameters of Fe^{3+} and Fe^{2+}, attributed to superparamagnetic magnetite.

The presence of widened sextets and doublets in the Mössbauer spectrum gives account of a distribution of particle sizes in the film, consistent with the SEM micrograph. The smallest particles can present superparamagnetic behavior, giving doublets in the spectrum because their magnetic moments relax in times less than the window time in Mössbauer spectroscopy of ^{57}Fe (10^{-8} s) [17]. On the other hand, the magnetic moments of the particles with sizes slightly higher than the superparamagnetic limit relax in times comparable with the window time of the technique, giving a distributed hyperfine magnetic interaction

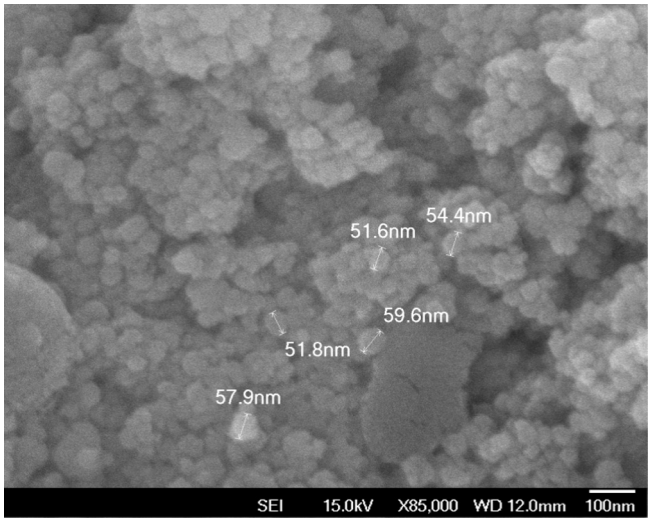

Fig. 8. SEM image of the film.

in all particles and producing widened sextets as those observed in Fig. 10.

4.7. Magnetization measurements

The room temperature hysteresis loop of the material of the film is presented in Fig. 11(a). A zoom of the central zone of the curve is presented in Fig. 11(b), in order to evidence the coercivity and remanence of the film.

The Table 2 presents the specific saturation magnetization M_s, specific remanent magnetization M_r and coercive magnetic field Hc extracted from the loop.

The film presents a magnetic soft behavior, the saturation begins at 500 Oe approximately and total saturation occurs at 4.5 kOe. The low value of the coercivity and remanence are consistent with the small particle size observed in the SEM images, where particles with dimensions less than 60 nm were observed. The doublets and widened sextets observed in the Mössbauer spectrum, as well as the particle size distribution observed in the SEM micrograph evidence that an important fraction of the particles in the film can be in superparamagnetic state due to small particle size effects. The saturation magnetization is less than that of a

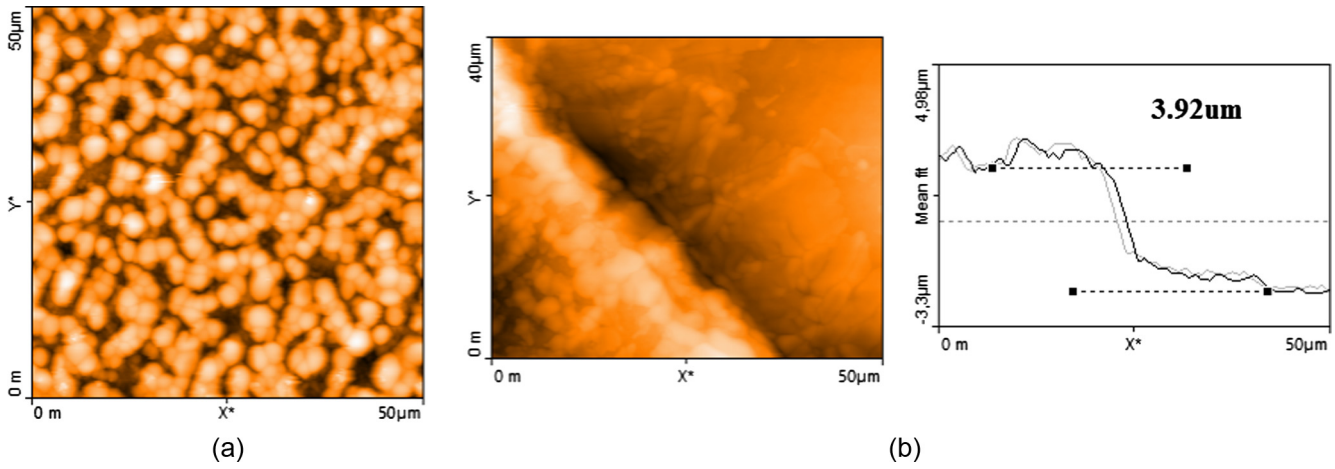

Fig. 9. a. AFM micrograph of the film, b. Estimation of the thickness of the film through a micrograph in the interfase film/substrate.

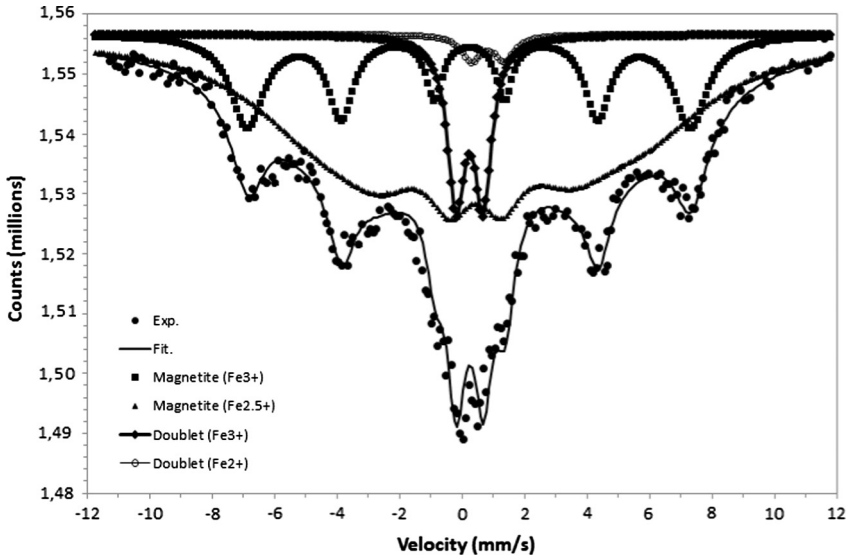

Fig. 10. Room temperature Mössbauer spectrum of the film.

Table 1
Mössbauer parameters of the iron phases identified in the films.

Sub-spectrum	Phase	B_{hf} (T)	IS (mm/s)	QS (mm/s)	W (mm/s)	A (%)
Sextet 1	Fe^{3+} (Fe_3O_4)	44.0 ± 0.2	0.35 ± 0.02	−0.02 ± 0.02	0.65 ± 0.02	20
Sextet 2	$Fe^{2.5+}$ (Fe_3O_4)	31.8 ± 0.2	0.64 ± 0.02	0.06 ± 0.02	1.83 ± 0.02	70
Doublet 1	Fe^{3+} (Fe_3O_4) Superparam.	—	0.36 ± 0.02	0.86 ± 0.02	0.66 ± 0.02	8
Doublet 2	Fe^{2+} (Fe_3O_4) Superparam.	—	0.96 ± 0.02	1.07 ± 0.02	0.75 ± 0.02	2

The convention of the spectral parameters is: B_{hf}: hyperfine magnetic field, IS: isomer shift relative to α-Fe, QS: quadrupole splitting, W: linewidth of the inner lines, A: spectral area.

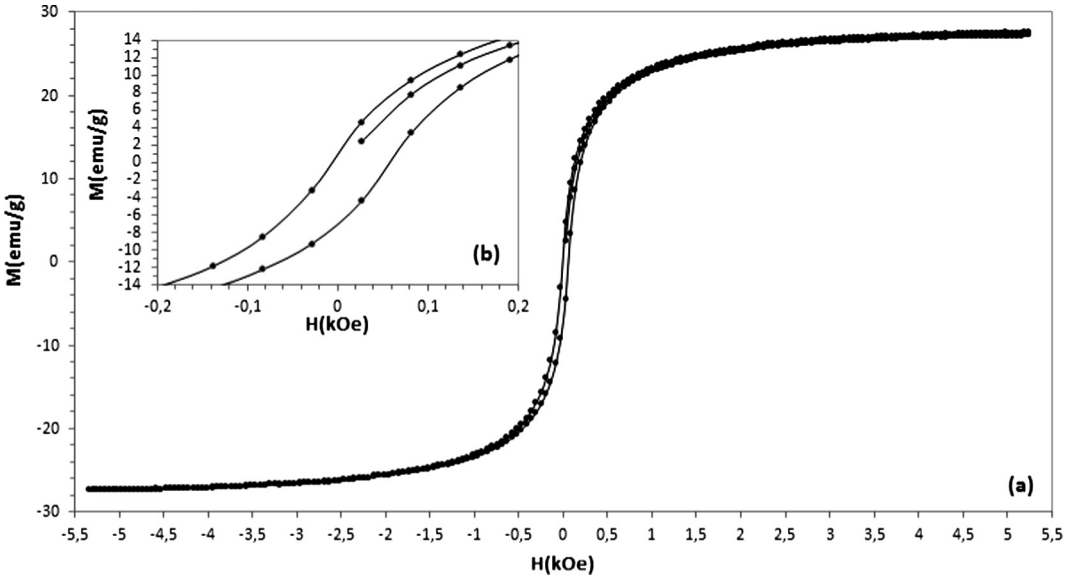

Fig. 11. Hysteresis loop of the film.

Table 2
Hysteresis parameters of the film.

M_s (emu/g)	M_r (emu/g)	H_C (Oe)
27.5 ± 0.2	3.8 ± 0.2	30 ± 2

crystalline and stoichiometric bulk magnetite, near to 92 emu/g [18], which is consistent with the nanoscale particle size, in which the sharp surface anisotropy effect reduces the net magnetic moment of the particles, lowering the total moment of the film. Other important factor which reduces the magnetization of the film is the presence of the residual polymer not decomposed during the thermal treatment. This polymer contributes to the sample mass but it does not contribute to the magnetic moment of the sample, which reduces the specific magnetization measured by VSM.

4.8. Voltage vs. Current measurements

Fig. 12 shows the behavior of the Voltage vs. Current applied to the film, by using currents in intervals of 0–200 nA. An

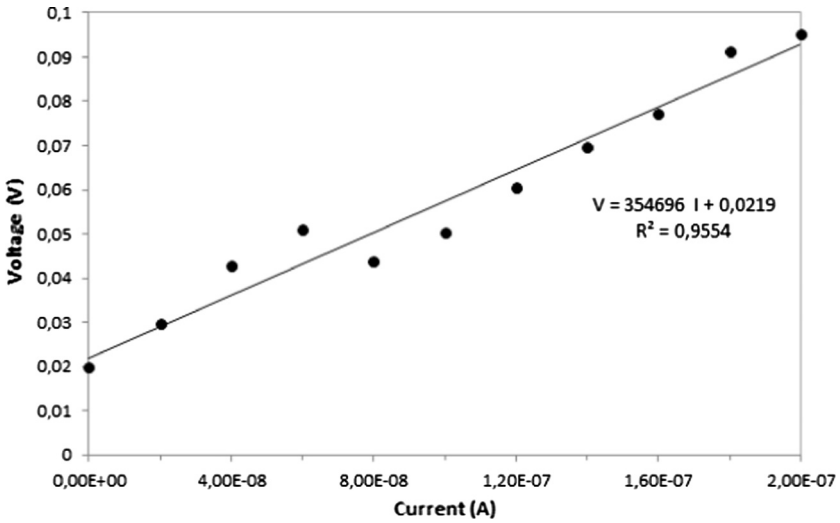

Fig. 12. Voltage vs. Current measurements by the four-point method.

approximately linear behavior was observed between voltage and the current, which indicates an ohmic nature of the films, being their electric resistance around to 355 kΩ. This value represents an average of the electric resistance of the film measured on a surface of 1cm^2 and a thickness around 4 μm estimated from AFM measurements, which can variate according to the dimensions considered for making these measurements. Given that the agarose employed in the synthesis is dielectric, the electric conductivity present in the films is related to the hopping current that is present by the electron thermally activated, which travels between ions Fe^{2+} and Fe^{3+} that occupy neighboring octahedra in the crystal structure of the magnetite. This effect is evidenced by the presence of the sextet attributed to an intermediate valence $Fe^{2.5+}$ in the Mössbauer spectrum discussed before. During the measurements it was observed that currents above 200 nA can produce damage in the film. Above this current the film behaves like an open circuit, with null conductivity.

5. Conclusions

We grew magnetite films by alkaline hydrolysis of Fe^{2+} and Fe^{3+} cations in an agarose hydrogel deposited on glass substrates. The presence of the polymer in the synthesis favors the formation of nanostructured particles on the surface of the substrate. After thermal treatment of the films at 120 °C, some residual polymer chains remained bonded to the surface of the magnetic particles, these chains can be used as support media for subsequent functionalization of the films in applications as sensing devices. The morphology of the particles of the films was quasi spherical, with particle sizes around 55 nm and with a distributed diameter. The films presented a soft magnetic response, low coercivity and a saturation magnetization whose value is around a third part of that of a bulk crystalline and stoichiometric magnetite. The films obtained by this method presented magnetic relaxation effects, evidenced by the coexistence of broaden sextets and doublets in the Mössbauer spectrum, indicating that a significant fraction of the particles are in the superparamagnetic limit of this technique. The films presented ohmic behavior for currents bellow 200 nA, indicating the presence of hopping effect due to the itinerant electron which travels between neighboring octahedra in the structure of magnetite. The magnetic and ohmic electrical response of the films obtained by this method make them promising for the construction of active sensing devices, where the magnetic and electrical properties of the films vary as a function of the elements adsorbed on surface of the magnetic particles.

References

[1] O.M. Lemine, K. Omri, B. Zhang, L. El Mir, M. Sajieddine, A. Alyamani, M. Bououdina, Sol-gel synthesis of 8 nm magnetite (Fe3O4) nanoparticles and their magnetic properties, Superlattices Microstruct. 52 (4) (2012) 793–799.

[2] W.B. Mi, J.J. Shen, E.Y. Jiang, H.L. Bai, Microstructure, magnetic and magneto-transport properties of polycrystalline Fe_3O_4 films, Acta Mater. 55 (2007) 1919–1926.

[3] S. Abe, S. Ohnuma, Magnetite thin films containing a small amount of Ge, Appl. Phys. Express 1 (11) (2008) 1113041–1113043.

[4] M. Alexe, M. Ziese, D. Hesse, P. Esquinazi, K. Yamauchi, T. Fukushima, U. Gösele, Ferroelectric switching in multiferroic magnetite (Fe_3O_4) thin films, Adv. Mater. 21 (44) (2009) 4452–4455.

[5] T. Furubayashi, Magnetite films prepared by reactive evaporation, J. Magn. Mag. Mater. vols. 1 of 2272–276 (SUPPL. 1) (2004) 1–2.

[6] H.S.W. Chang, C.-C. Chiou, Y.-W. Chen, S.R. Sheen, Synthesis, characterization and magnetic properties of Fe_3O_4 thin films prepared via a sol-gel method, J. Solid State Chem. 128 (1) (1997) 87–92.

[7] N.J. Tang, W. Zhong, H.Y. Jiang, X.L. Wu, W. Liu, Y. Du, Nanostructures magnetite (Fe_3O_4) thin films prepared by sol-gel method, J. Magn. Magn. Mater. 282 (1–3) (2004) 92–95.

[8] M. Chiba, K. Morio, Y. Koizumi, Microstructure and magnetic properties of iron oxide thin films by solid reaction, J. Magn. Magn. Mater. 239 (2002) 457–460.

[9] L.J. Van der Pauw, A method of measuring specific resistivity and Hall effect of discs of arbitrary shapes, Philips Res. Rep.: J. Theor. Exp. Res. Phys., Chem. Allied Fields 13 (1) (1958) 1–9.

[10] Emine. Yalçın, Kültiğin. Çavuşoğlu, Glutaraldehyde cross-linked agarose carriers: design, characterization and insulin release behaviour, Turk. J. Biochem. 33 (4) (2008) 148–153.

[11] Masakuni. Tako, The principle of polysaccharide gels, Adv. Biosci. Biotechnol. 6 (2015) 22–36.

[12] Mounir. Maaloum, Nadine. Pernodet, Bernard. Tinland, Agarose gel structure using atomic force microscopy: Gel concentration and ionic strength effects, Electrophoresis 19 (10) (1998) 1606–1610, http://dx.doi.org/10.1002/elps.1150191015.

[13] D. Mihir Oza, Ramavatar Meena, Kamalesh Prasada, P. Paulb, A.K. Siddhanta, Functional modification of agarose: a facile synthesis of a fluorescent agarose–guanine derivative, Carbohydr. Polym. 81 (2010) 878–884.

[14] S. Aliramaji, A. Zamanian, Z. Sohrabijam, Characterization and synthesis of magnetite nanoparticles by innovative sonochemical method, Procedia Mater. Sci. 11 (2015) 265–269.

[15] H. Lepp, Stages in the oxidation of magnetite, Am. Mineral. 42 (1957) 679–681.

[16] R. Vandenberghe, E. De Grave, P.M.A. De Bakker, On the methodology of the analysis of Mössbauer spectra, Hyperfine Interact. 83 (1994) 29–49.

[17] Q.A. Pankhurst, J. Connolly, S.K. Jones, J. Dobson, Application of magnetic nanoparticles in biomedicine, J. Phys. D: Appl. Phys. 36 (2003) R167–R181.

[18] F. Fajaroh, H. Setyawan, W. Widiyastuti, S. Winardi, Synthesis of magnetite nanoparticles by surfactant-free electrochemical method in an aqueous system, Adv. Powder Technol. 23 (2012) 328–333.